

Stellar Multiplicity via Speckle Interferometry with the 3.6 m Devasthal Optical Telescope

Km Nitu Rai^{*1}, Neelam Panwar¹, Jeewan C Pandey¹, T S Kumar¹, Subrata Sarangi^{2, 3},
and Prasenjit Saha⁴

¹*Aryabhatta Research Institute of Observational Sciences, Manora Peak, Nainital 263129, India.*

²*School of Applied Sciences, Centurion University of Technology and Management, Odisha-752050, India.*

³*Visiting Associate, Inter-University Centre for Astronomy and Astrophysics, Post Bag 4, Ganeshkhind, Pune 411 007, Maharashtra, India.*

⁴*Physik-Institut, University of Zurich, Winterthurerstrasse 190, 8057 Zurich, Switzerland.*

Abstract

Conventional ground-based optical telescopes, even those with large apertures, primarily observe stars, close binaries, and multiple systems as unresolved point sources through photometric measurements. Spectroscopy can identify multiple stellar components within a system, but both techniques are fundamentally limited in resolving stellar surfaces and providing direct angular separations. Although photometric and spectroscopic observations yield critical information on magnitudes/flux, metallicities, and orbital properties, complementary high-angular-resolution methods are required to constrain additional system characteristics, including angular orbital parameters, model-independent distances, radii, and stellar masses. The limitations of these two methods arise due to the Diffraction Limit of the telescopes and atmospheric turbulence. Speckle Interferometry (SI) is a clever and affordable method for ground-based telescopes to work around atmospheric turbulence. In this work, we utilize the speckle images obtained by the 3.6 m DOT and demonstrate the capability of SI to resolve binary systems, measure their orbital separations, and determine their position angles. For systems with faint companions where conventional analysis fails, we employ Bayesian inference to model speckle patterns and estimate orbital parameters with high precision. These results establish the effective methodology for using a medium-sized, 4-m class telescope like the DOT as a high-resolution stellar interferometer and demonstrate the potential of speckle interferometry as a powerful technique to advance optical interferometric studies within Indian astronomy.

Keywords: Diffraction limited Resolution, Speckle Interferometry, Binary Star

1 Introduction

The Earth's atmosphere poses a significant challenge to high-spatial resolution astronomical imaging. Due to vast interstellar distances and the ef-

fects of Earth's atmospheric turbulence, stellar objects appear as unresolved point sources to the naked eye and as blurred images through ground-based optical telescopes. Even large-aperture telescopes are fundamentally limited in achieving their theoretical diffraction-limited resolution. The 3.6-meter Devasthal Optical Telescope (DOT) has a theoretical resolving power of approximately 0.035 arc-seconds at 500 nm. Median seeing of ~ 1 arcsec of site prevents the telescope's ability to resolve binary stars with sep-

^{*}E-mail: niturai201296@gmail.com

arations < 1 arcsec Sagar et al. (2020). However, observations of binary stars at DOT in December 2015 demonstrated a minimum resolvable separation of ~ 0.4 arc-seconds Sagar et al. (2019) under the best seeing conditions.

To overcome these limitations, several high-resolution imaging techniques have been developed over the past few decades. These include adaptive optics Hardy (1998); Tyson et al. (2022), lucky imaging Fried (1978), and various interferometric methods such as speckle masking Lohmann et al. (1983) and Speckle Interferometry (SI; Weigelt et al. 1983; Scott et al. 2018). Among these, SI has proven to be a particularly effective technique for achieving near-diffraction-limited resolution using ground-based telescopes.

First introduced by Labeyrie (1970) and theoretically grounded in the photon correlation principles established by Hanbury Brown & Twiss (1957), SI captures a series of short-exposure images of the target system, of the order of milliseconds, thus effectively “freezing” atmospheric turbulence. These exposures exhibit high-frequency spatial information as speckle patterns. However, these patterns also embody low-frequency structural and orbital information about the star and the stellar system, as the particular case may be. The structural and orbital information of the stellar object can be recovered through postprocessing of these short-exposure images using standard Fourier Transform methods Labeyrie (1977). Graphical representation of the number of objects in the stellar system can also be extracted from the autocorrelation of the power spectrum of these images Decker (1977). However, this method is not applicable for full image reconstruction. The speckle masking method was initially developed to reconstruct the exact image of the objects Weigelt (1977); Weigelt & Wirtzner (1983). Currently, bi-spectrum or triple correlation is also in application for reconstruction of a real image of the target Lohmann et al. (1983).

Originally developed to resolve bright binary systems McAlister et al. (1989), now SI has evolved to study a wide range of astrophysical targets, including exoplanet detection, using advanced detectors and sophisticated data processing algorithms Horch et al. (2009); Scott et al. (2021); Howell et al. (2021); Bo-

drito et al. (2025). State-of-the-art instruments at telescopes such as the 3.5-meter WIYN Observatory Howell et al. (2024), the 4.1-meter SOAR Observatory Ziegler et al. (2021); Tokovinin et al. (2024), and the 8.1-meter Gemini telescopes Lester et al. (2021); Scott et al. (2021) have successfully used SI to characterize intermediate-separation binaries. Most recently, SI observations with Gemini North led to the detection of a second companion around Betelgeuse Howell et al. (2025), highlighting SI as a high-resolution technique for resolving multiple stellar systems.

The Devasthal Optical Telescope (DOT) with its 3.6m Ritchey-Chrétien system has undertaken an ambitious project of establishing an SI pipeline dedicated to observation and review of binary and other multi-star systems. As a pilot, in this study, we utilize the speckle images of two binary star systems obtained from the 3.6-m DOT Kumar et al. (2025) to demonstrate speckle interferometry. The large aperture and the stable tracking system of DOT offer significant advantages for photon-limited, high-resolution imaging. We apply Fourier-based analysis for data reduction and the autocorrelation method to obtain the graphical representation of the diffraction pattern characteristic of for the graphical representation of binary star systems. This traditional method works for 52 Orionis, providing a clear picture of the binary nature with two different sets of short-exposure image data. However, for 10 Arietis, the straightforward Fourier-power spectrum and autocorrelation method fails to recover a resolved characteristic two-lobe diffraction pattern. For this case and for possible similar cases involving binary systems with faint secondaries (like 10 Arietis), that this project might encounter in its survey, we have explored the use of Bayesian inference techniques. We construct Bayesian models using the thousands of recorded short-exposure images and use them to estimate the orbital separation of binaries, along with other parameters. These two binaries have a separation of more than one arc-second and can be resolved with typical medium-sized classical optical telescopes. As stated above, the objective of this work is to initiate the institution of a pipeline project of Speckle Interferometry (SI) technique for Dev-

asthal Observatory, Nainital, and inspire to extend its applicability to all three telescopes: the Devasthal Optical Telescope (DOT), the Devasthal Fast Optical Telescope (DFOT), and the Sampurnanand Telescope (ST). In this work, we do not attempt to reconstruct the full images of the target systems. The selected binaries serve as test cases to benchmark SI-based measurements with DOT, complementing conventional photometric and spectroscopic observations. This study lays the groundwork for future real-time SI implementations and advanced data analysis pipelines, thereby contributing to the development of optical interferometric expertise within India’s astronomical community.

This paper is organized as follows. Section 2 sketches the basic theoretical concepts underlying the SI technique. Section 3 presents, in reverse order, an outline of the Bayesian Model constructed in this work using the short-exposure images and introduces other estimated and relevant system priors. Section 4 refers to specifications of the 3.6-m DOT and the procedure adopted to record the short-exposure data. Section 5 describes the two target stellar systems and presents, in sequence, the results of this pilot study. In Section 6, we discuss the implications and prospects of SI as a back-end instrument for the DOT and other Indian optical telescopes at large.

2 Theoretical Background for Speckles

Ground-based optical observations are fundamentally limited by time-dependent and random phase distortions in the incoming wavefront from stellar sources. However, over very short timescales, typically a few tens of milliseconds, the phases across the arriving wavefronts can be considered constant. Signals recorded with a high-speed detector within such intervals capture barely discernible coherence patterns and diffraction-limited information encoded in the speckles. Subsequent analysis of the speckle frames recorded over a short duration time interval enables the recovery of diffraction-limited details and, in the case of binaries, the determination of orbital param-

eters as well.

2.1 Diffraction Limit and Atmospheric Constraints

The diffraction-limited angular resolution at wavelength λ for a telescope of objective diameter D is given by

$$\theta \approx 1.22 \frac{\lambda}{D}. \quad (1)$$

In the absence of an atmosphere, a point source would produce an Airy diffraction pattern, whose form depends on the source’s structure. A single star yields a circular Airy disk, whereas a binary star system produces interference fringes modulated on the Airy pattern. In practice, atmospheric turbulence distorts the incoming wavefront and blurs the Airy pattern, thereby preventing direct observation of fine structure.

2.2 Fourier Analysis of Speckle Patterns

Speckle Interferometry (SI) circumvents atmospheric blurring by recording short-exposure frames of the distorted wavefront. Each frame contains a random speckle pattern, but its Fourier Transform (FT) retains the low-frequency information of the stellar object while treating the atmospheric perturbations as multiplicative high-frequency noise. Since each frame contains only a partial sampling of the photon distribution, the Fourier domain representation of a single speckle image returns blurred array patterns, which also vary over time. However, by averaging the FT over many short-exposure frames, the atmospheric noise averages out, and the object’s spatial frequency content becomes more clearly discernible. In the case of binary stars, this averaging recovers characteristic fringe patterns in the Fourier domain.

2.3 Autocorrelation: Graphical Representation

Following the Wiener–Khinchine theorem [Khinchine \(1934\)](#), the ensemble-averaged power spectrum

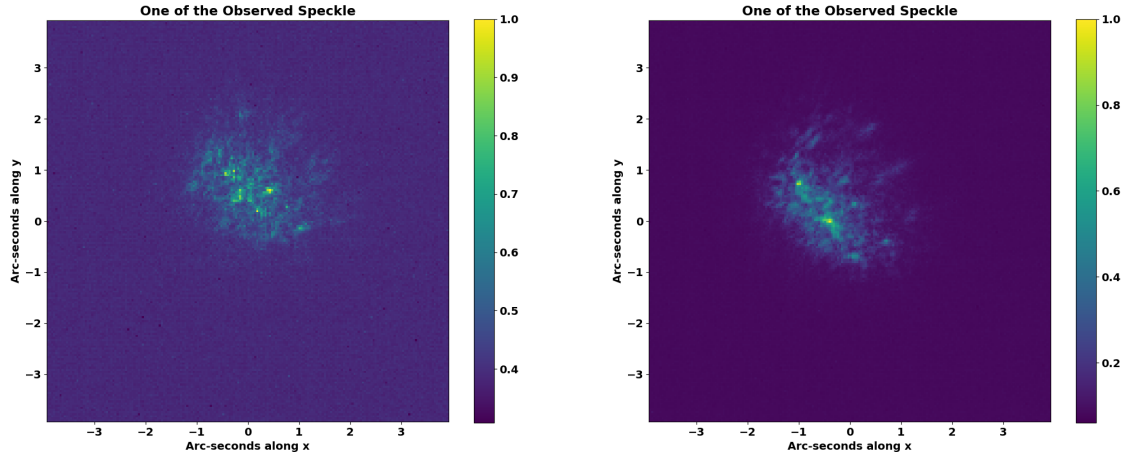


Figure 1: The left and right panels show the speckle patterns of 52 Orionis with 2 ms and 10 ms exposure times, respectively.

(squared modulus of the FT) of the speckle frames can be inverse Fourier transformed to yield the autocorrelation of the object's diffraction-limited image. For a binary star, the autocorrelation function displays a central bright spot accompanied by two symmetrically located secondary peaks corresponding to the projected separation of the components. This provides a direct graphical signature of the binary nature of the target. While the autocorrelation approach reveals separations and position angles, complete image reconstruction requires higher-order statistics, such as triple correlation or bi-spectrum analysis.

3 Modeling of Speckle Patterns

In the case of a fainter binary companion, the conventional diffraction-limited imaging techniques may fail due to the insufficient photon flux from the secondary component. To overcome this limitation, we employ a Bayesian inference model that incorporates not only the Fourier transform of the short-exposure speckle patterns but also the explicit modeling of the

corresponding autocorrelation over time.

The speckle intensity distribution for a single star is defined as

$$I(u) = I_1 \left[2 \frac{J_1(u)}{u} \right]^2 \quad (2)$$

J_1 represents the first-order Bessel function of the first kind. I_1 is the brightness of star and u is defined as

$$u = \frac{\pi D \theta}{\lambda} = \frac{\pi \theta}{a} \quad (3)$$

with observational wavelength λ , telescope diameter D , and the scale parameter $a = \lambda/D$. This parameter accounts for the diffraction limit as well as atmospheric and instrumental effects that manifest through the effective point-spread function (PSF). θ is the angular position of the distribution on the observational plane.

The intensity distribution for a binary star system on the detector plane at position can be modeled as

$$I(u_1, u_2) = \left[2 \frac{J_1(u_1)}{u_1} \right]^2 + b \left[2 \frac{J_1(u_2)}{u_2} \right]^2, \quad (4)$$

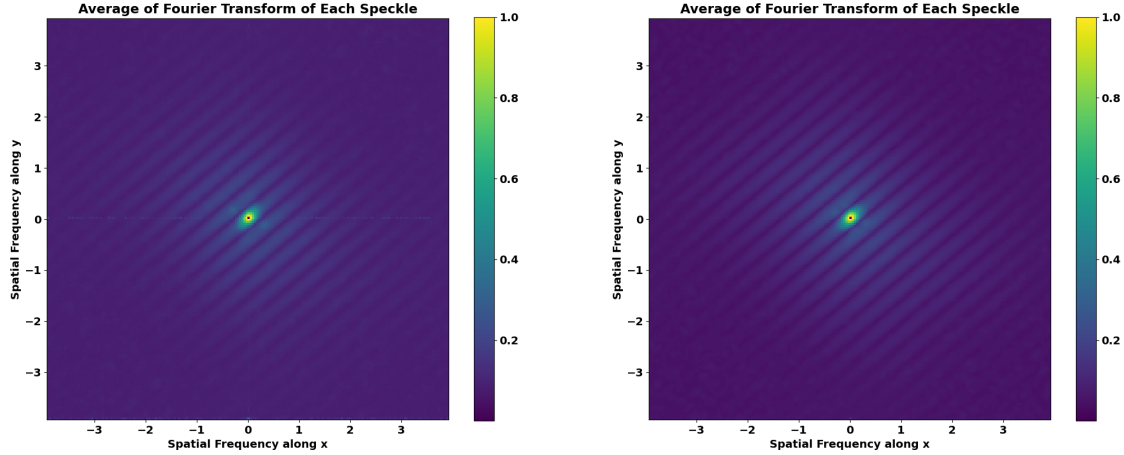


Figure 2: The left and right panels show the fringe patterns of 52 Orionis obtained by averaging over the Fourier power spectra of 1000 short-exposure image frames with exposure times of 2 ms and 10 ms, as shown in Fig. 1. The square root of both data sets has been taken here for clear visualization.

where $b = I_2/I_1$ denotes the brightness ratio of the two stellar components and

$$u_2 = \frac{\pi(\theta + \Delta\theta)}{a} \quad (5)$$

$\Delta\theta$ stands for the angular separation between the stars and is resolved into Cartesian components according to

$$\Delta\theta_x = \Delta\theta \cos(\phi), \quad (6)$$

$$\Delta\theta_y = \Delta\theta \sin(\phi), \quad (7)$$

where ϕ is the position angle of the binary system on the sky in degrees. In this framework, the key parameters to be estimated include the position angle ϕ , brightness ratio b , projected separation $\Delta\theta$, and the PSF scaling factor a . These parameters are inferred by fitting the modeled speckle distribution to the observed data within a Bayesian statistical approach, thereby enabling the recovery of orbital information even in cases of binary stellar systems where the secondary component is faint.

3.1 The Likelihood and Estimation of Parameters

Let us assume that the autocorrelation of the observed speckle patterns, denoted as $A_{obs}(s)$ with s representing the sky coordinate, follows a Gaussian noise with standard deviation σ_s . We use pixel-to-pixel variation in intensities to calculate σ_s . The observed data is modeled according to the autocorrelation $A(s)$, after computation of the inverse Fourier Transform of the power spectrum of equation 4. The next step is to estimate the underlying binary star parameters by fitting the model to the observed data. We adopt a Bayesian framework in which the likelihood function quantifies the probability of obtaining the measured autocorrelation given a set of model parameters $\omega = \{b, \Delta\theta, \phi, a\}$. The likelihood function is defined according to

$$\ln P(\{A_{obs}(s)\}|\alpha, \omega) = -\frac{1}{2} \sum_s \frac{(A_{obs}(s) - \alpha A(s, \omega))^2}{\sigma_s^2} \quad (8)$$

where α is a Nuisance parameter and can be marginalized out as (please see section 4.2 of Rai et

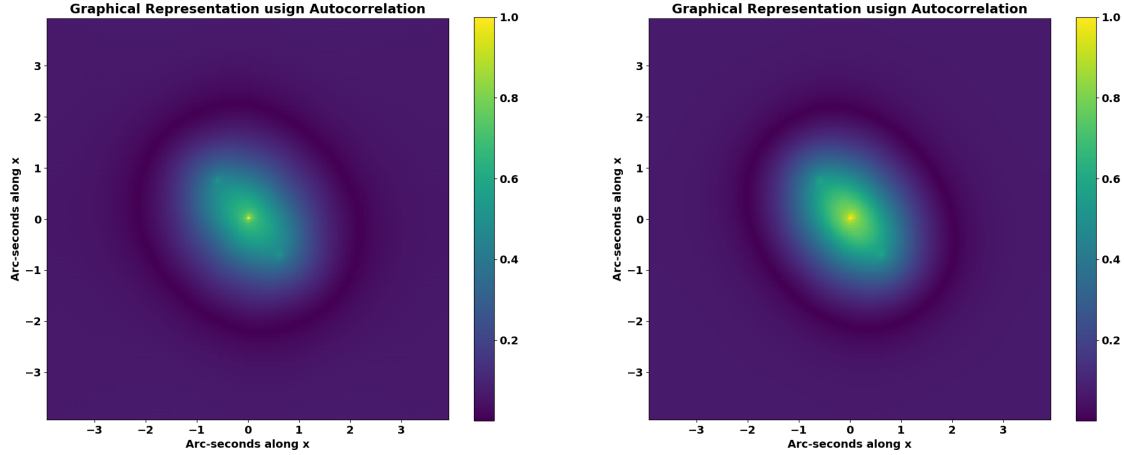


Figure 3: The left and right panels show the graphical representation of 52 Orionis after taking the inverse Fourier transform of the power spectrum (autocorrelation) of Fig. 2, respectively.

al. (2021)) $A(s, \omega)$ represents the autocorrelation of the modeled data with varied sets of model parameters ω . With the marginalization incorporated, we have the likelihood function reduced to

$$\ln P(\{A_{obs}(s)\}|\omega) = \frac{G^2}{2W} - \frac{1}{2} \ln W \quad (9)$$

where,

$$G = \sum_s \sigma_s^{-2} A_{obs}(s) A(s, \omega) \quad (10)$$

and the scalar product of the model with itself

$$W = \sum_s \sigma_s^{-2} A(s, \omega)^2 \quad (11)$$

We use equation 9 for sampling and Parameter estimation, which is carried out by maximizing the posterior probability, which combines the likelihood with prior information on the parameters through Bayes' theorem:

$$P(\omega | A_{obs}(s)) \propto P(A_{obs}(s)|\omega) P(\omega). \quad (12)$$

Here $P(\omega)$ represents the priors, which can incorporate physical constraints such as positivity of brightness ratios, realistic ranges for separations, or previously known orbital information.

We use the dynesty package to sample the data and to estimate the parameter Speagle (2020). This package provides not only the most probable values of the binary parameters but also robust estimates of their uncertainties and correlations. The resulting posterior distributions allow us to quantify the confidence in measurements of orbital separation, position angle, brightness ratio, and PSF scaling, even in cases where the secondary component is faint and conventional approaches fail.

4 Observations of Speckles from Binaries

Observations of speckle patterns from binary systems were conducted using a high-speed CMOS camera mounted on the 3.6-m DOT. This setup enables short-exposure imaging at millisecond (2, 10, and

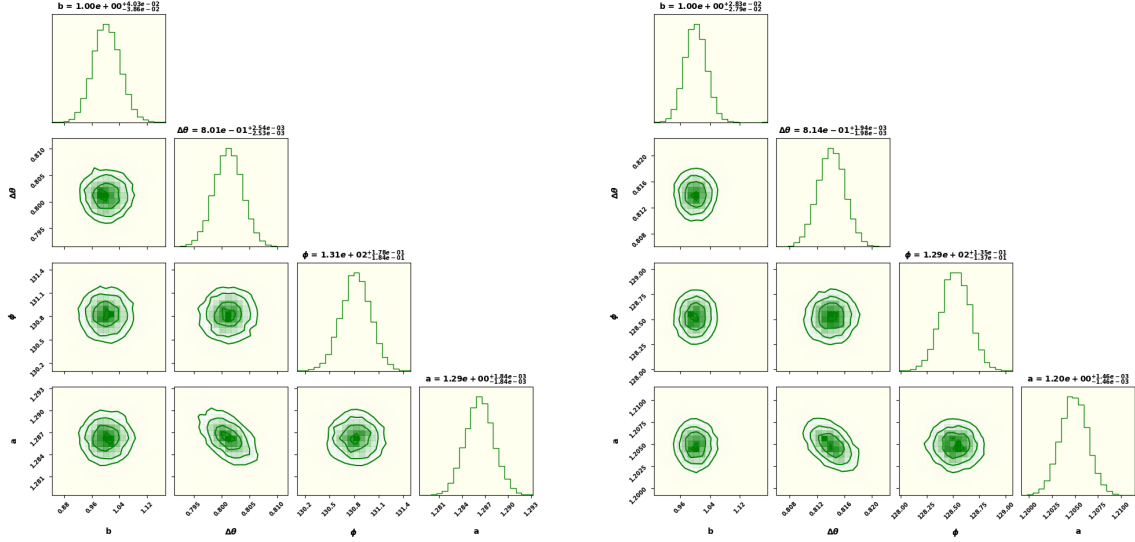


Figure 4: The left and right panels show the results of parameter estimation of 52 Orionis using the Bayesian modeling of autocorrelation (Fig. 3) of speckle patterns for 2 ms and 10 ms exposure times (one example shown in Fig. 1), respectively.

100) timescales, essential for freezing atmospheric turbulence and retrieving diffraction-limited information. The 3.6-m DOT, located at Devasthal, Nainital, is a Ritchey–Chrétien optical configuration with an effective focal ratio of $f/9$ Kumar et al. (2018). The telescope has three instrument ports, a main port (axial port), and two side ports. It is equipped with multiple back-end instruments, including SPIM Nainital (2023), ADFOSC Omar et al. (2019), TANSPEC Sharma et al. (2022), and TIRCAM2 Baug et al. (2018), which support photometry and low-resolution spectroscopy. For the present study, the CMOS detector sCMOS (2022) was mounted at the main port of the DOT to facilitate speckle interferometry observations.

Speckle interferometric observations were carried out for a selected sample of binary star systems using short-exposure imaging sequences. For each target, several data cubes were acquired with exposure times of 2 ms, 10 ms, and 100 ms, and with frame counts ranging from 1,000 to 10,000, to optimize the signal-to-noise ratio (SNR) under varying atmospheric con-

ditions. The use of high-cadence imaging preserved the fine-scale, diffraction-limited speckle patterns essential for Fourier-domain analysis and accurate recovery of binary parameters. In the subsequent analysis, only 1,000 frames were utilized, as the sensitivity gain beyond this number was found to be negligible for 10-ms exposures.

5 The Target Sources and Parameter Estimation

In this work, we focus on two binary systems, 10 Arietis (10 Ari) and 52 Orionis (52 Ori), where one or both components are main-sequence stars. Having obtained their speckle observations, we now process them following the procedure outlined in Section 2. The analysis procedure involves:

- Computing the Fourier transform of each short-exposure image frame,
- Obtaining the power spectrum of each frame,

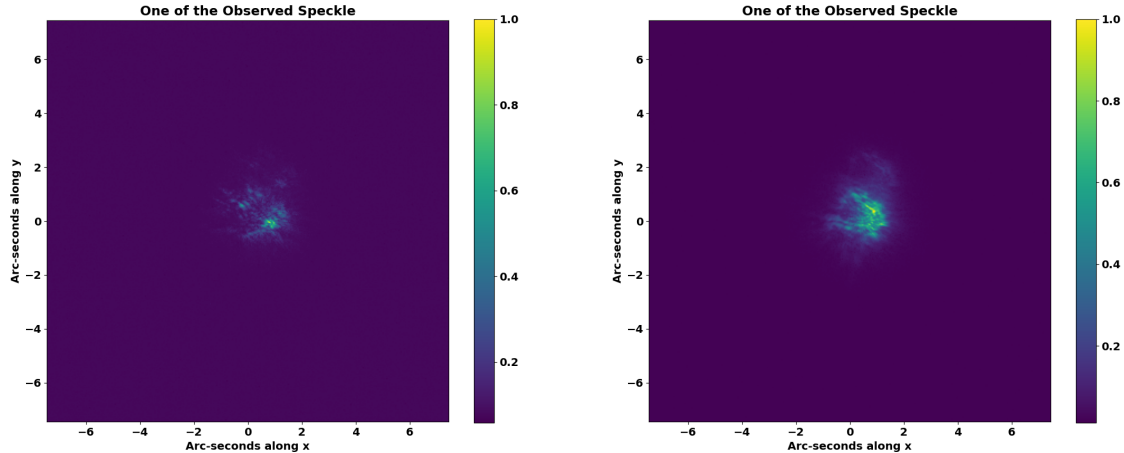


Figure 5: The left and right panels show the speckle patterns of 10 Arietis with 10 ms and 100 ms exposure times, respectively.

- Averaging the power spectra over multiple frames,
- Applying the inverse Fourier transform on the averaged power spectrum to compute the autocorrelation of the source.

While this standard procedure yields a clear visualization for the binary nature of 52 Ori, it does not provide a reliable resolution for 10 Ari, as this binary has a faint companion of magnitude 7.95 [Eggleton & Tokovinin \(2008\)](#). To overcome this, we employ Bayesian inference to model the speckle patterns and estimate the system parameters with improved accuracy (as described in Section 3). The σ_s value is calculated using the pix-to-pix variation in intensity of autocorrelation. We notice a small variation in the value of σ_s for each dataset and for each of the binary systems. Ignoring the variation over different data sets, and choosing the system-specific values as 0.02 for 52 Ori and 0.01 for 10 Ari.

5.1 52 Orionis

52 Ori is a well-known binary star system composed of two main-sequence stars located at a distance of approximately 479.41 light-years from the Sun. Speckle interferometric observations were performed for this system using multiple short-exposure sequences to capture the speckle patterns under varying temporal resolutions. For the processing, analysis, and extraction of model parameters of system 1,000 data frames are taken for each exposure setting from the recorded speckle patterns. Figure 1 illustrates one of the representative speckle patterns obtained with exposure times of 2 milliseconds (left panel) and 10 milliseconds (right panel).

As described in Section 2, the Fourier transform of these individual image frames exhibits speckle patterns and the blurred diffraction structure of the source. However, following the analysis procedure indicated above, the random atmospheric phase noise is effectively suppressed, thereby recovering the underlying diffraction features of the binary system. This effect is clearly visible in Figure 2, where straight interference fringes confirm the binary nature of 52 Ori.

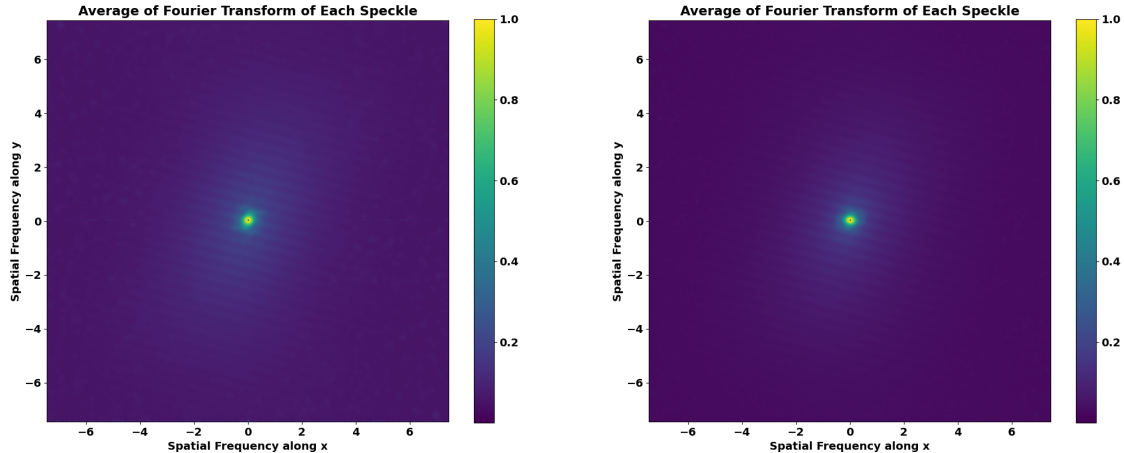


Figure 6: The left and right panels show the fringe pattern of 10 Arietis obtained by averaging over the Fourier power spectra of 1000 short-exposure image frames with exposure times of 10 ms and 100 ms, as shown in Fig. 1. As the companion of 10 Ari is very faint. We have taken the square root of the fringes here for clear visualization.

The inclination of these fringes with respect to the horizontal axis indicates the position angle of the binary components relative to the telescope’s projected position.

To visualize the binary configuration and estimate the orbital parameters, the power spectrum was computed and subsequently subjected to an inverse Fourier transform (auto-correlation), as discussed in Section 2. The resulting autocorrelation map, shown in Figure 3, reveals a characteristic three-lobed structure—one central peak flanked symmetrically by two side peaks—signifying the binary nature of the system. The separation between the central and side peaks provides a direct measure of the angular separation of the components. At the same time, their orientation relative to the x-axis yields the position angle, subject to a 180° ambiguity. According to Fig. 3, the $\Delta\theta_x$ and $\Delta\theta_y$ separation are around 0.65 and 0.75 arc-second with inclination $\phi \approx 130^\circ$. It results in a separation of both stars in 52 Ori $\theta \approx 0.99$ arc-second. This angle is resolvable by DOT with its

existing optics and associated instrumentation. However, a detailed examination and discussion of the resolving power of DOT and other telescopes is beyond the scope of this work and shall be pursued in later projects. We shall continue with the task of extracting information on binary star systems using Speckle Interferometry data.

Bayesian inference-based model fitting was performed on the autocorrelation data (Figure 3) of 52 Ori. The resulting posterior distributions, presented as corner plots in Figure 4 for both exposure times (corresponding to Figure 1), show the inferred parameters: the brightness ratio ($b \approx 1$), angular separation ($\Delta\theta \approx 0.80$ in arc-seconds), position angle ($\phi \approx 130$ in degrees), and the Bessel function parameterization ($a \approx 1.2$ per arc-second), which quantifies the loss in visibility due to observational and instrumental effects. The posterior distributions also quantify the associated parameter uncertainties, all of which are well constrained.

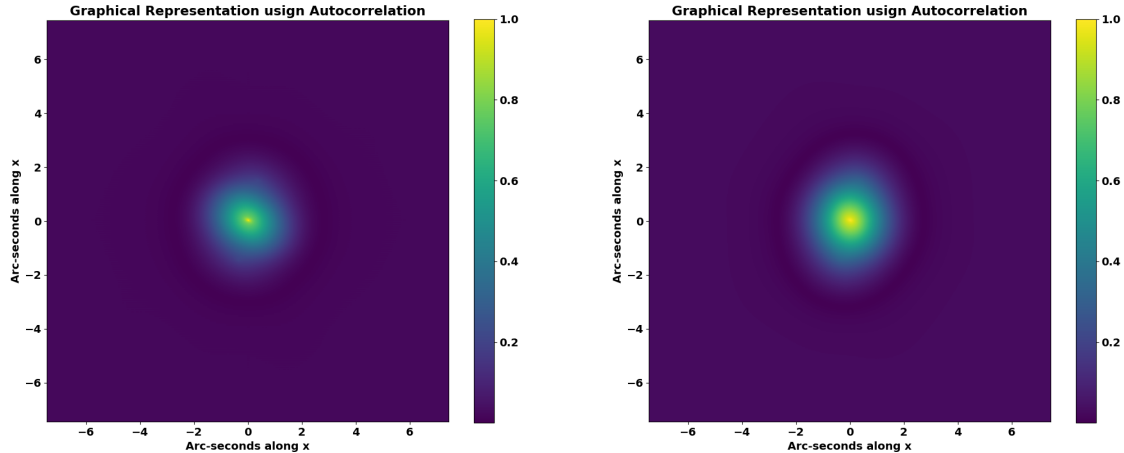


Figure 7: The left and right panels show the graphical representation of 10 Arietis after taking the Fourier transform of the power spectrum of Fig. 2, respectively. However, the side dots are not visible clearly while having the fringe nature in the diffraction pattern shown in Fig. 6.

5.2 10 Arietis

10 Ari is a binary star system with an orbital period of approximately 325 years, located at a distance of about 159 light-years from the Sun. The system consists of a bright F-type main-sequence primary star and a much fainter secondary companion. We recorded speckle patterns of this binary system with exposure times of 10 ms and 100 ms, acquiring 1000 data frames for each case. Representative speckle patterns for both exposure times are shown in Fig. 5 (left and right panels, respectively). Both of these datasets are subjected to Fourier processing. The square root of the power spectrum of these two data sets is presented in Fig. 6. The fringes are faint, barely visible around the central peak. This is due to the low brightness of the secondary component in the 10 Ari system. However, it provides the information about the angle $\phi \approx 77^\circ$. The inverse Fourier transform of the power spectrum does not produce well-defined side lobes around the central peak, as shown in Fig. 7 (left and right panels).

For binaries with faint companions, model-based

fitting of speckle data often yields more robust results than traditional Fourier-based analyses. Motivated by this, we adopted a Bayesian inference framework and performed parameter estimation using Dynesty on the autocorrelation functions of the speckle frames (Fig. 7). The corresponding posterior distributions are shown in Fig. 8 for both exposure durations associated with the speckle images in Fig. 5. The inferred parameters include the component brightness ratio (b), angular separation ($\Delta\theta$, in arcseconds), position angle (ϕ , in degrees), and the Bessel-function PSF scaling parameter (a , per arcsecond). Together, these quantities provide both the quality of the observational data and the configuration of the binary system.

A few noteworthy trends emerge from the two datasets (10 ms and 100 ms exposures):

- The 100 ms data exhibit noticeable autocorrelation between the inferred brightness ratio and angular separation, indicating systematics introduced by longer exposures. However, the parameters have been estimated accurately and show

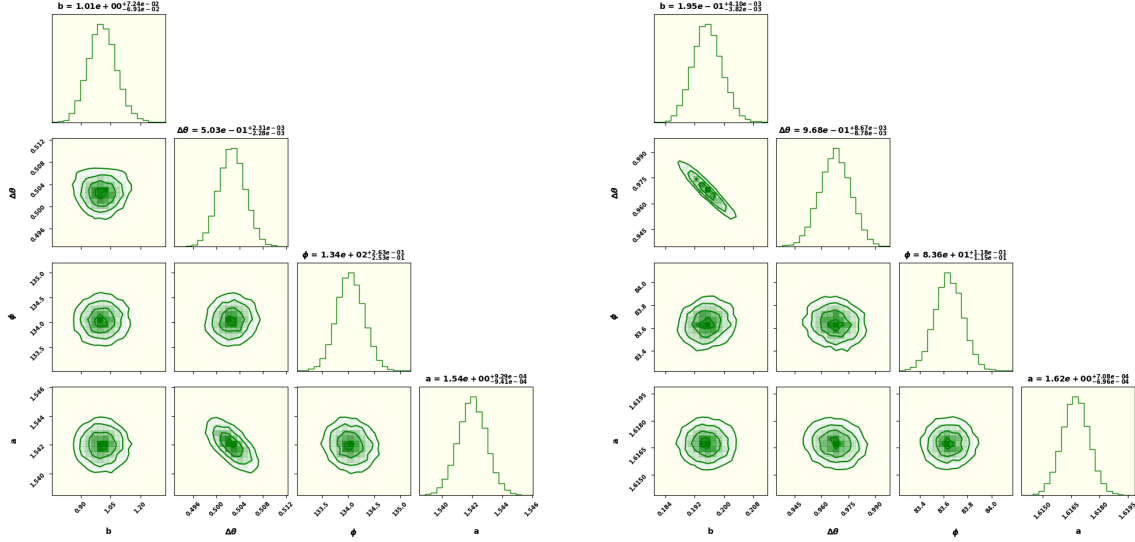


Figure 8: The left and right panels show the results of parameter estimation of 10 Arietis using the Bayesian modeling of autocorrelation of the speckle patterns for 10 ms and 100 ms exposure time, respectively.

consistency with the autocorrelation result.

- The parameter estimates from the 10 ms frames are substantially less constrained, suggesting that very short exposures may not provide sufficient SNR for reliable inference.

These aspects will be investigated further using the recently concluded November 2025 DOT observations of faint binary systems, which are expected to provide higher-quality data for testing the stability and reliability of the Bayesian fitting approach.

6 Conclusion

Photometry and spectroscopy have long been the primary back-end instruments at the Devasthal Optical Telescope (DOT), providing crucial insights into stellar objects. However, achieving high angular resolution for multi-star systems requires additional instrumentation. This study demonstrates that integrating Speckle Interferometry (SI) into DOT represents a significant advancement, complementing its existing capabilities.

In this work, we present the first successful implementation of SI on DOT, demonstrating its ability to resolve a binary system with a bright companion using Fourier transformation and autocorrelation techniques. While the detection of faint companions remains challenging in another binary star system, the application of Bayesian inference to model speckle patterns shows great promise in estimating orbital parameters with high precision. These results highlight the potential of SI to achieve angular resolution with reduced uncertainties, establishing a foundation for future observational campaigns targeting multiple, binary, and single-star systems with DOT.

Additionally, the present study underscores the importance of revisiting SI as a powerful observational tool in India. Although earlier developments at the Vainu Bappu Observatory (VBO), Kavalur, demonstrated the feasibility of SI [Saha et al. \(1999\)](#), the lack of a dedicated observational campaign limited the scientific outcomes [Saha et al. \(2002\)](#). Our findings revive this prospect by demonstrating the effectiveness of SI on modern optical facilities, thereby encouraging Indian astronomers to expand its use for

stellar studies and foster collaborative efforts to advance high-resolution astronomy in the northern sky.

Acknowledgements

One of the authors (SS) gratefully acknowledges the computing facilities and the local hospitality offered to him by the Inter-University Center for Astronomy and Astrophysics (IUCAA), Pune, India under its Visiting Associate Program during the preparation and finalization of this manuscript.

References

- Baug, T., Ojha, D. K., Ghosh, S. K., et al. 2018, *Journal of Astronomical Instrumentation*, 7, 1850003
- Bodrito et al., T. 2025, in *Proceedings of the IEEE/CVF Conference on Computer Vision and Pattern Recognition (CVPR)*, 1230–1240
- Decker, A. J. 1977, *Analytical procedure for evaluating speckle-effect instrumentation*
- Eggleton, P. P. & Tokovinin, A. A. 2008, *Monthly Notices of the Royal Astronomical Society*, 389, 869
- Fried, D. L. 1978, *Journal of the Optical Society of America*, 68, 1651
- Hanbury Brown, R. & Twiss, R. Q. 1957, *Proceedings of the Royal Society of London Series A*, 242, 300
- Hardy, J. W. 1998, *Adaptive Optics for Astronomical Telescopes*
- Horch et al., E. P. 2009, *The Astronomical Journal*, 137, 5057
- Howell et al., S. B. 2021, *The Astronomical Journal*, 161, 164
- Howell et al., S. B. 2024, *The Astronomical Journal*, 167, 258
- Howell et al., S. B. 2025, *The Astrophysical Journal Letters*, 988, L47
- Khintchine, A. 1934, *Mathematische Annalen*, 109, 604
- Kumar, T. S., Kumar, B., Ray, S., & Shah, M. 2025, manuscript in preparation
- Kumar et al., B. 2018, *Bulletin de la Societe Royale des Sciences de Liege*, 87, 29
- Labeyrie, A. 1970, *Astronomy and Astrophysics*, Vol. 6, p. 85 (1970), 6, 85
- Labeyrie, A. 1977, in (Elsevier), 47–87
- Lester et al., K. V. 2021, *The Astronomical Journal*, 162, 75
- Lohmann, A. W., Weigelt, G., & Wirtzner, B. 1983, *Applied Optics*, 22, 4028
- Lohmann et al., A. W. 1983, *Applied Optics*, 22, 4028
- McAlister et al., H. A. 1989, *The Astronomical Journal*, 97, 510
- Nainital, D. O. 2023, *SPIM on the 3.6m DOT*, accessed: 2025-10-30
- Omar, A., Kumar, T. S., Reddy, B. K., Pant, J., & Mahto, M. 2019, *Current Science*, 116, pp. 1472
- Rai et al., K. N. 2021, *MNRAS*, 507, 2813
- Sagar, R., Kumar, B., & Omar, A. 2019, *Current Science*, 117, 365
- Sagar, R., Kumar, B., & Sharma, S. 2020, *Journal of Astrophysics and Astronomy*, 41, 33
- Saha et al., S. 1999, *Experimental Astronomy*, 9, 39
- Saha et al., S. 2002, *Bulletin of the Astronomical Society of India*, Vol. 30, p. 677-678 (2002), 30, 677
- sCMOS, M. 2022, *Marana sCMOS-Andor*, accessed: 2025-10-30
- Scott et al., N. J. 2018, *Publications of the Astronomical Society of the Pacific*, 130, 054502

- Scott et al., N. J. 2021, *Frontiers in Astronomy and Space Sciences*, 8, 138
- Scott et al., N. J. 2021, *Frontiers in Astronomy and Space Sciences*, 8, 716560
- Sharma, S., Ojha, D. K., Ghosh, A., et al. 2022, *Publications of the Astronomical Society of the Pacific*, 134, 085002
- Speagle, J. S. 2020, *Monthly Notices of the Royal Astronomical Society*, 493, 3132
- Tokovinin et al., A. 2024, *The Astronomical Journal*, 168, 28
- Tyson et al., R. K. 2022, *Principles of adaptive optics* (CRC press)
- Weigelt, G. 1977, *Optics Communications*, 21, 55
- Weigelt, G. & Wirtzner, B. 1983, *Opt. Lett.*, 8, 389
- Weigelt et al., G. 1983, *Optics Letters*, 8, 389
- Ziegler et al., C. 2021, *The Astronomical Journal*, 162, 192